Electronic Supplementary Information

Ultrasensitive Label-Free Electrochemical Biosensor for MicroRNA-21 Detection based on 2′-O-methyl modified DNAzyme and Duplex-Specific Nuclease Assisted Target Recycling

Xi Zhang [a], Dongzhi Wu [a], Zhijing Liu [a], Shuxian Cai [a],Yanping Zhao [a], Mei Chen [a], Yaokun Xia [a], Chunyan Li [a], Jing Zhang* [b], Jinghua Chen* [a]

a Department of Pharmaceutical Analysis, Faculty of Pharmacy, Fujian Medical University, Fuzhou, Fujian Province 350108, P R China.

b The Ministry of Education Key Laboratory of Biopesticide and Chemical Biology, and College of Life Sciences, Fujian Agriculture and Forestry University, Fuzhou, Fujian Province 350002, P R China.

1. Experimental parts

Reagents. HPLC-purified miRNAs, were purchased from Takara Biotechnology Co., Ltd. (Dalian, China). All DNA oligonucleotides were synthesized by Sangon Biotech Co. (Shanghai, China), and their base sequences were illustrated in Table S1. The concentrations were quantified by OD260 based on their individual absorption coefficients. DSN was purchased from Evrogen Joint Stock Company (Moscow, Russia). RNase inhibitor was purchased from Takara Biotechnology Co., Ltd. (Dalian, China). Tris-(hydroxymethyl) aminomethane was purchased from Cxbio Biotechnology Co. Ltd. (Denmark). Ethylenediaminetetraacetic acid (EDTA), Hexaammineruthenium (III) chloride (RuHex, 98 %), mercaptohexanol (MCH) and tris (2-carboxyethyl) phosphine hydrochloride (TCEP) were purchased from Sigma-Aldrich (USA). TMB/H_2O_2 and hemin were purchased from Sigma-Aldrich (St. Louis, MO, USA), respectively. The stock solution of hemin (5 mM) was prepared in DMSO, stored in the dark at -20 ^{0}C and

diluted to the required concentrations with Tris-HCl buffer solutions. All chemicals were of analytical grade.

Table S1 Details of the DNA sequences

Signal probe (Sp)	5′-HS-TTTTTT***ATTGGGAGGGATTGGGTGGG*****TCAACATCAGTCTGATAAGCTA**-3′
miR-21 (M)	5′- UAGCUUAUCAGACUGAUGUUGA-3′
single-base mismatched miRNA(M1)	5′- UA**C**CUUAUCAGACUGAUGUUGA-3′
single-base mismatched probe(M2)	5′-UAG CUU AUC A**C**ACUG AUG UUG A-3′
single-base mismatched probe(M3)	5′- UAGCUUAUCAGACUGAUGUU**C**A-3′
single-base mismatched probe(M4)	5′-UAG CUU AUC A**A**ACUG AUG UUG A-3′;
single-base mismatched probe(M5)	5′-UAG CUU AUC A**T**ACUG AUG UUG A-3′
miR-141	5′-UAACACUGUCUGGUAAAGAUGG-3′
let-7d	5′-AGAGGUAGUAGGUUGCAUAGUU-3′
Control probe (Cp)	5′-HS-TTTTTT***ATTCCCATCGATAGTGTGAG*****TCAACATCAGTCTGATAAGCTA**-3′

The italic bold letters represent the 2′-O-methyl modified G-rich DNAzyme sequence or control sequence. The bold letters indicate target-binding sequence. The underlined bold letters indicate the mismatched position.

Solutions.

Hybridization buffer was the mixture of 100 mM NaCl and 10 mM TE (pH 7.4). DNA immobilization buffer was the mixture of 10 mM TE, 10 mM TCEP and 1000 mM NaCl. Washing buffer solution was 100 mM NaCl and 10 mM PB solution (pH 7.4). All solutions were prepared with MilliQ water (18.2 MΩ).

Electrochemical measurements.

All electrochemical measurements were performed by using CHI 660D Electrochemical Workstation (CH Instrument, USA). The electrochemical system consisted of a working electrode (a gold disk electrode modified with Sp), a platinum wire as the auxiliary electrode, and a reference electrode (Ag/AgCl). Cyclic voltammetrys (CVs) were carried out at a scan rate of 100 mV/s. Amperometric detection was preformed with a fixed potential of 100 mV and the steady state was usually reached and recorded within 100 s. The electrochemical impedance spectra (EIS) was recorded in the frequency range of 0.1 kHz~100 Hz with a sampling rate of 12 points per decade in 10 mM Tris-HCl-10 mM $[Fe(CN)6]^{4-/3-}$ solution (pH 7.0). The biased potential was 0.21V (versus Ag/AgCl) and the amplitude was 5.0 mV. A Nyquist plot (Z_{re} vs Z_{im}) was drawn to analyze the impedance results. The circular dichroism (CD) spectra were studied based on the Jasco J-810 circular dichroism spectropolarimeter (Tokyo, Japan).

DNA self-assembly, Hybridization and the Nicking Reaction at gold electrode.

The whole fabrication process of the biosensor is outlined in Fig. 1. A gold disk electrode (2 mm diameter, GE, the surface area of gold electrode was 0.043 cm^2 calculated by the integration of the cathodic peak in 0.1M H_2SO_4 [1-2]) was firstly polished to obtain mirror surface with 0.05 μm alumina powder, followed by sonication in ethanol and water for 5 min respectively. Then the GE was electrochemically cleaned to remove any remaining impurities. After being dried with nitrogen, the electrode was immediately used for DNA immobilization. 5 μL of 2 μM Sp solution was first spread on the pre-cleaned gold electrode surface for 2 hours in the 100 % humidity. Next, this electrode was immersed in 1 mM MCH for 1 hour to remove the nonspecific DNA adsorption, leading to optimizing the orientation of Sp to make hybridization easier. The DNA surface density could be measured with chronocoulometry (CC) as previously described.[3] Then, 5 μL of the hybridization solution containing complementary miR-21, single-base mismatch M1-M5 or other miRNA (miR-141 and let-7d) was placed on the DNA self-assembly monolayer of Sp modified

GE for 1 h at room temperature, respectively. After hybridization, the GE was extensively rinsed with washing buffer solution and dried under a stream of nitrogen gas. Afterward, the sensor was incubated in a solution of 0.2 U DSN reaction buffer (50 mM Tris-HCl, pH 8.0, 5 mM $MgCl_2$, 1 mM DTT, 20 U RNase inhibitor) at 60 °C (such temperature could facilitate faster hybridization and subsequent dissociation of DNA in the reaction buffer [4]). After a specified period of time, the electrodes were rinsed with wash buffer and dried under a stream of nitrogen gas. Finally, the above electrodes were incubated in the hemin solution to form the G-Quadruplex-hemin DNAzyme at 25 ℃, and detected in the TMB/H_2O_2 solution by electrochemical measurements.

2. RESULTS AND DISCUSSION

Characterization of 2′-O-methyl modified Sp *by circular dichroism*

In order to improve the sensitivity of the sensor, we modified the G-rich fragments of Sp with 2′-O-methyl to facilitate the formation of perfect fine-tuning parallel G-quadruplexes and promote peroxidase activity. It is well known to all, CD spectroscopy is a very useful tool for the characterization of G-quadruplexes. Signature CD spectra have been reported for many DNA structures including dsDNA and G-quadruplex species.[5] Here, we used CD to investigate the feasibility of 2′-O-methyl modification. As shown in Fig. S1b, in PB buffer containing K^+, the CD spectrum of Sp gave a clear signal of parallel G-quadruplexes with a positive peak at 264 corresponding to base stacking, and a negative peak at around 240 nm corresponding to helicity.[5] While the CD spectrum of 2′-O-methyl modified Sp exhibited a significant augment of positive peak at 264 nm, it indicated that 2′-Omethyl modification increased structural and thermal stability of G-quadruplex.

Insert of Fig. S1 showed the photographs of TMB/H_2O_2 system in the presence of Sp or 2′-O-methyl modified Sp with K^+ and hemin. The 2′-O-methyl modified Sp exhibited more obvious color change compared to Sp, displaying drastically enhanced peroxidase activity. The enhanced

peroxidase activity of 2′-O-methyl modified Sp was attribute to hydrophobic 2′-O-methyl, which improved structure stability and enhanced hydrophobic interaction between the G-quadruplex and hemin.

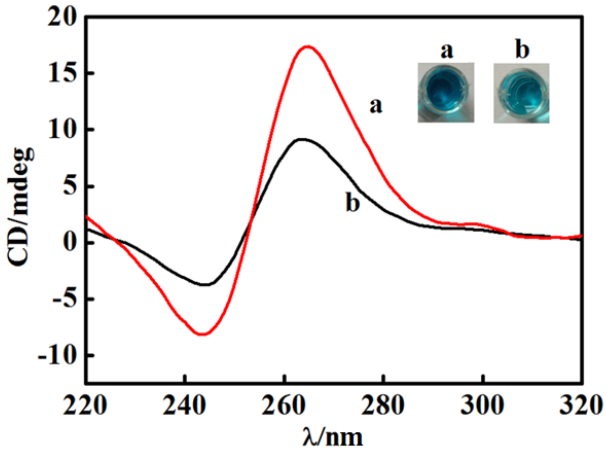

Fig. S1. CD spectra of 4 μM 2′-O-methyl modified Sp (a) and 4 μM Sp (b) in PB buffer containing K^+ and hemin. Insert: Photographs of TMB oxidation TMB/H_2O_2 system taken after 5 min of reaction at room temperature with K^+ in the presence of hemin+2′-O-methyl modified Sp (a), hemin+Sp (b).

Enzymatic activity comparison of DNAzyme immobilized on GE and free in solution.

To investigate whether the enzymatic activity of DNAzyme was negatively affected by immobilization of the oligonucleotides on GE surface, CV signals of TMB substrate in DNAzyme solution (PB buffer containing K^+, hemin and 2′-O-methyl modified Sp) and at DNAzyme modified GE were all measured. As shown in Fig. S2 A-c, we can see two pairs of redox peaks when the bare electrode was immersed into TMB substrate. Upon DNAzyme solution addition, a prominent catalytic reduction peak was found (Fig. S2A-b), reflecting the DNAzyme efficiently catalyzed the reduction of hydrogen peroxide with the help of TMB (an electroactive co-substrate). At the same time, the solution colour observed with naked eyes gradually changed from colourless

(inset c) to blue (inset b). Then different DNA modified GE were compared in the same TMB substrate. The peak current of Sp/MCH/GE (Fig. S2A-d) and Sp-miR-21/MCH/GE (Fig. S2A-f) were close to that of bare electrode. Even if add hemin on the above modified electrodes (Sp/MCH/GE+ hemin and Sp-miR-21/MCH/GE+hemin), there were no obvious change of current signal (Fig. S2A-e and Fig. S2A-g). This phenomenon demonstrated Sps could not bind hemin to form the G-quadruplex DNAzyme due to the steric-hindrance effect, resulting in a poor catalytic current signal. Upon DSN and hemin addition, we can find a prominent catalytic reduction peak appeared in CV of Sp-miR-21/MCH/GE (Fig. S2A-a) and the solution colour changed to blue too (see inset a), which demonstrated a nearly unaltered enzymatic activity compared to DNAzyme free in solution. That was because only 2′-Omethyl modified G-rich nucleic acid sequences remained on the surface GE after many strand-scission cycles. Therefore, with the addition of hemin, 2′-Omethyl modified G-rich sequences bound hemin to form the G-quadruplex-hemin DNAzyme, which catalyzed the H_2O_2-mediated oxidation of TMB, giving rise to an enzymatically amplified electrochemical current signal. All above results demonstrated the enzymatic activity of DNAzyme immobilized on GE was close to DNAzyme free in solution, and our biosensor indeed worked as expected.

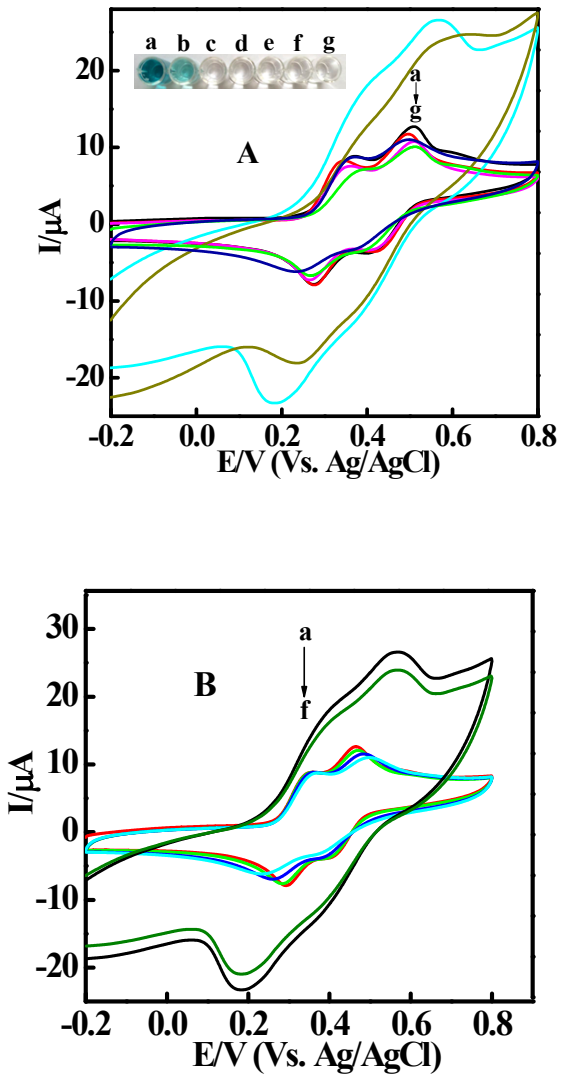

Fig. S2 A) CVs of TMB substrate at different GE: (a) Sp-miR-21/MCH/GE + DSN+ hemin, (b) bare GE + DNAzyme solution, (c) bare GE, (d) Sp/MCH/GE, (e) Sp/MCH/GE+ hemin, (f) Sp-miR-21/MCH/GE, (g) Sp-miR-21/MCH/GE+hemin. Inset: the corresponding photograph of TMB substrate at different GE. **B)** CVs of TMB substrate at different GE: Sp-miR-21/MCH/GE +DSN+hemin in PBS buffer (a) or in serum sample (b), bare GE in PBS buffer (c) or in serum sample (d) and Cp-miR-21/MCH/GE+DSN+hemin in PBS buffer (e) or in serum sample (f).

Evaluation of the signal amplification ability of DNAzyme

In order to further evaluate the signal amplification ability of DNAzyme, a control probe (Cp), which couldn't form G-quadruplex, was selected to compare with Sp. As shown in Fig. S2B, after the same procedures including DNA self-assembly, hybridization and the DSN cleavage reaction, Cp-miR-21/MCH/GE+DSN+hemin show a poor catalytic current signal (close to that of bare electrode, curve c and d) in both standard and complicated serum samples (curve e and f). It demonstrated that only Sp, which could form G-quadruplex, can bind hemin to form G-quadruplex-hemin DNAzyme with horseradish peroxidase-like activity and effectively catalyze the H_2O_2-mediated oxidation of TMB (curve a and b).

CVs of RuHex and EIS characterization in the different stage of the electrochemical biosensor.

Previous studies have demonstrated that RuHex can bind to DNA by electrostatic interaction since the DNA backbone has negative charge. In order to further test whether indeed our biosensor works as expected, the CV behaviour of RuHex was investigated at different stages of the biosensor preparation. As shown in Fig. S3, two pairs of peaks corresponding to the reduction and oxidation of RuHex could be observed at a relatively dilute concentration (5 μM) at Sp/MCH/GE (Fig. S3A, curve a). Because the peak separation was close to zero and peak currents were linearly proportional to scan rates, peak 1 was ascribed to electrostatically binding of RuHex to the DNA surface and reflected the amount of DNA on the electrode surface, while peak 2 reflected $[Ru(NH_3)_6]^{3+}$ diffusion to MCH.[3] When Sp/MCH/GE was incubated in the miR-21 solutions, Sps hybridized with miR-21 to form a double helix structure. As a result, the amount of the RuHex electrostatically bound to the GE surface increased with a much higher current signal (Fig. S3A, curve b), while the peak 2 was almost neglectable. After Sp-miR-21/MCH/GE being incubated in DSN (Fig. S3A, curve c), there was a sharp decrease in current signals of peak 1, while that of

peak 2 increased. It could be attributed to the hydrolysis of DSN against Sps, which led to the decrease of negative charges on the GE surface as well as the dramatic decrease of binding amount of RuHex. All above results of CVs demonstrated that our biosensor indeed worked as expected.

EIS was investigated at different stages of the biosensor preparation. As shown in Fig. S3B, compared with the bare GE (curve a), the Sp/MCH/GE showed a larger electron-transfer resistance (Ret) (curve d), mainly due to the electrostatic repulsion between negative charges of the DNA backbone and the $Fe(CN)_6^{3-/4-}$. Upon addition of hemin, DSN, or DSN+hemin, respectively, Sp/MCH/GE+hemin (curve e), Sp/MCH/GE+DSN (curve f) and Sp/MCH/GE+DSN+hemin (curve g) showed no obvious change of Ret compared to that of Sp/MCH/GE, reflecting no G-quadruplex formed. However, upon addition of target miR-21, Sp could hybridize with it to form DNA-RNA hybrids (Sp-miR-21/MCH/GE), resulting in an increase of negative charges as well as the value of Ret (curve h). The addition of hemin could not enhance the value of Ret (Sp-miR-21/MCH/GE+ hemin, curve i) because no G-quadruplex was formed due to steric-hindrance effect from DNA-RNA hybrids. Nevertheless, after the addition of DSN, the value of Ret sharply decreased (Sp-miR-21/MCH/GE+ DSN, curve b). This is because the strong hydrolysis preference of DSN for DNA in DNA-RNA hybrids selectively hydrolyze the target recognition sequence of Sp, resulting in only 2′-O-methyl modified G-rich sequence part of Sp remaining on the electrode surface. At the same time, miR-21 was dissociated to hybridize with a new, un-hydrolyzed Sp. Ultimately, only 2′-O-methyl modified G-rich fragments of Sps remain on the electrode surface, resulting in a sharp decrease of negative charges as well as the value of Ret. Upon addition of hemin, the 2′-O-methyl modified G-rich sequences could bind

hemin to form compact G-quadruplex. Hence, the penetration of $Fe(CN)_6^{3-/4-}$ through the DNA monolayer was hindered, which in turn led to the increase of Ret (Sp-miR-21/MCH/GE+DSN+hemin, curve c). The results of EIS were consistent with that of CV signals in TMB substrate, indicating that our biosensor indeed worked as our expected.

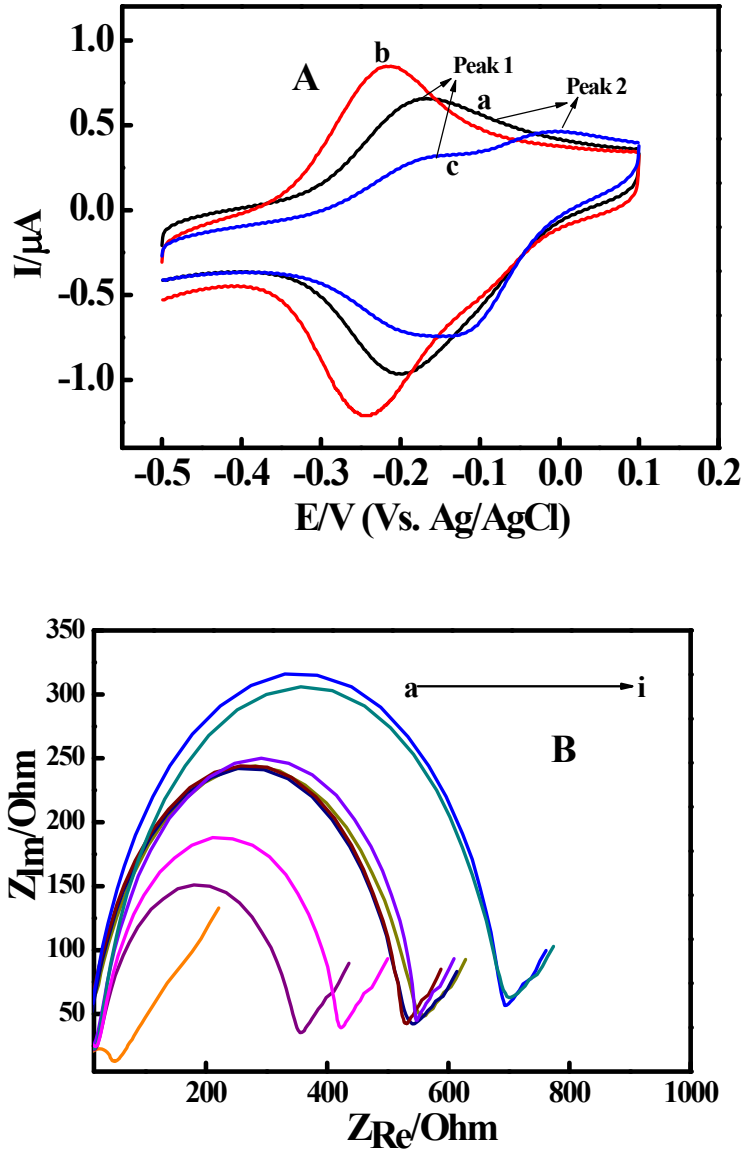

Fig. S3 A) CVs for a 10 mM Tris–HCl buffer (pH 7.4) containing 5 μM RuHex obtained at the Sp/MCH/GE (a), Sp-miR-21/MCH/GE (b), and Sp-miR-21/MCH/GE being incubated in DSN (c).

B) Electrochemical impedance spectra of different modified electrodes: bare GE (a); Sp-miR-21/MCH/GE+DSN (b), Sp-miR-21/MCH/GE+DSN+hemin (c), Sp/MCH/GE (d), Sp/MCH/GE+hemin (e), Sp/MCH/GE+DSN (f); Sp/MCH/GE+DSN+hemin (g), Sp-miR-21/MCH/GE (h), Sp-miR-21/MCH/GE+ hemin (i).

Optimization of Experimental Conditions

The factors including buffer type, pH of the buffer, concentration of hemin, and reaction time between hemin and rudimental G-rich nucleic acid sequences were examined in detail. The results showed the DNAzyme displayed its maximum catalytic activity at the following conditions: PBS buffer at pH 7.4, 0.5 μM hemin and 25 min of reaction time.

The sensitivity of the Electrochemical biosensor

Table S2. The detection limit for miR-21 of this method and some different detection methods

Method	Detection limit	Refs.
Fluorescence	100 fM	4 (Yin et al., 2012)
Fluorescence	5 pM	6 (Degliangeli et al., 2014)
Fluorescence	300 fM	7 (Xi et al., 2014)
Electrochemistry	67 fM	8 (Dong et al., 2012)
Electrochemistry	10 fM	9 (Wang et al., 2012)
Electrochemistry	6 fM	10 (Yin et al., 2012
Electrochemistry	10 fM	11 (Gao and Peng, 2011)
Electrochemistry	60 fM	12 (Yin et al., 2012)
Colorimetry	10 nM	13(Zhang et al., 2009)

Piezoelectric cantilever biosensors	4 fM	14 (Johnson and Mutharasan, 2012)
Fluorescence	2.1 fM	15 (Dong et al., 2012)
Electrochemistry	8 aM	This work

Detection of miR-21 in real serum sample

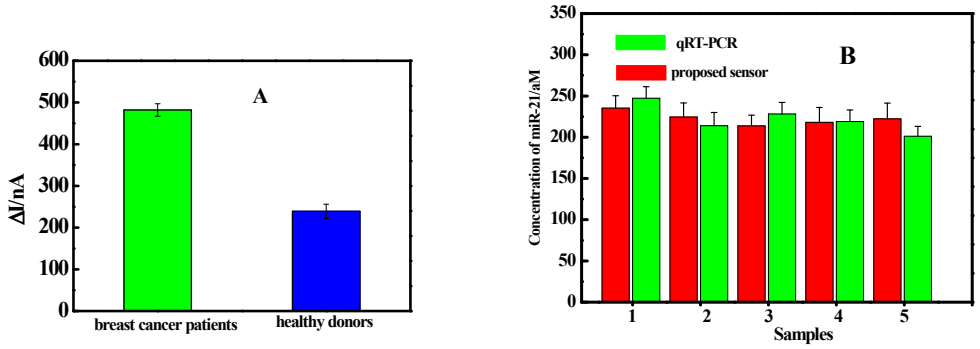

Fig. S4 A) Current-time responses comparison of target miR-21 in the serum of breast cancer patients and healthy donors. Error bars represent the standard error in data collected from five samples. B) Bars represent the concentration of miRNA-21 in serum samples detected by the proposed sensor (red bars) and qRT-PCR (green bars), respectively. Error bars represent standard deviations for measurements taken from at least five independent experiments.

The kinetics of enzymatic reaction

We examined the kinetics of enzymatic reaction by real-time monitoring the increase of the current signal. As shown in Fig. S5, the value increased for approximately 25 min before reaching a plateau corresponding to complete

hydrolyzation of all immobilized Sps. So the value was chosen for further studies.

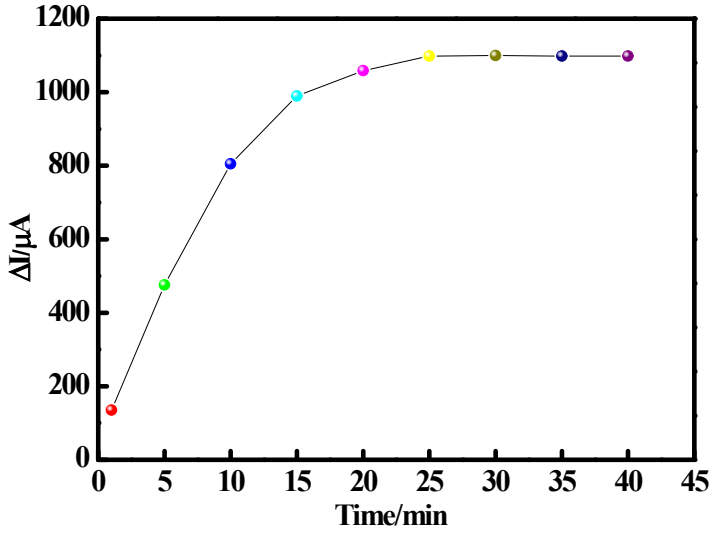

Fig. S5 Real-time monitoring of detection system containing 500 aM miR-21 and 0.2 U DSN.

References

1 Trasatti, S., Petrii, O. A. J. Electroanal. Chem. 1992, **327**, 353.

2 Filho, G.T., Dall' Antonia, L.H., Jerkiewicz, G. J. Electroanal. Chem. 1997, **422**, 149.

3 Lao, R., Song, S., Wu, H., Wang, L., Zhang, Z., He, L., Fan, C. Anal. Chem. 2005, **77**, 6475.

4 Yin, B. C., Liu, Y. Q., Ye, B. C. J. Am. Chem. Soc. 2012, **134**, 5064.

5 Balagurumoorthy, P., Brahmachari, S. K. J. Biol. Chem. 1994, **269**, 21858.

6 Degliangeli, F., Kshirsagar, P., Brunetti, V., Pompa, P. P., Fiammengo, R. J. Am. Chem. Soc. 2014, **136**, 2264.

7 Xi, Q., Zhou, D. M., Kan, Y. Y., Ge, J., Wu, Z. K., Yu, R. Q. Jiang, J. H. Anal. Chem. 2014, **86**, 1361.

8 Dong, H., Jin, S., Ju, H., Hao, K., Xu, L. P., Lu, H., Zhang, X. Anal. Chem. 2012, **84**, 8670.

9 Wang, J., Yi, X., Tang, H., Han, H., Wu, M., Zhou, F. Anal. Chem. 2012, **84**, 6400.

10 Yin, H., Zhou,Y., Chen, C., Zhu, L., Ai, S., Analyst. 2012, **137**, 1389.

11 Gao, Z., Peng,Y. Biosens. Bioelectron. 2011, **26**, 3768.

12 Yin, H., Zhou, Y., Zhang, H., Meng, X., Ai, S. Biosens. Bioelectron. 2012, **33**, 247.

13 Zhang, Y., Li, Z., Cheng, Y., Lv, X. Chem. Commun. 2009, **22**, 3172.

14 Johnson, B. N., Mutharasan, R., Anal. Chem. 2012, **84**, 10426.

15 Dong, H., Zhang, J., Ju, H., Lu, H., Wang, S., Jin, S., Hao, K., Du, H., Zhang, X. Anal. Chem. 2012, **84**, 4587.